

**Tenth International Congress
on Sound and Vibration
7–10 July 2003 • Stockholm, Sweden**

TENSION IN FLUTTERING FLAGS

Peter M. Moretti

Oklahoma State University
School of Mechanical & Aerospace Engineering
Stillwater, OK 74078-5016, USA

<http://www.mae.okstate.edu/Faculty/moretti/moretti.html>

Abstract

When a flag flutters, tension is dynamically induced by the two-dimensional vibratory motion. The dynamic process, involving centrifugal forces due to the curved path of the trailing edge, is similar to the whipping of an oscillating rope, and accounts for most of the drag-force observed at the flagpole attachment (luff). Conversely, the induced tension, combined with the curvature of the fabric, opposes the pressure forces from the flow field and extracts momentum from it.

In order to estimate post-critical flag and panel flutter amplitudes, it is necessary to compute the structural stiffening due to dynamically induced tension.

Tension in typical flag flutter motion, consisting of a traveling wave growing in amplitude as it progresses towards the trailing edge, is obtained by approximate analysis, using a Computer Algebra System. The general P.D.E. of motion is obtained from Hamilton's principle.

The time-averaged tension depends on the square of the velocity amplitude of the oscillating fabric. The distribution of time-averaged tension is shown for a typical flag flutter motion. An estimate of the tension fluctuations is developed. The fluctuations are small (relative to the average tension) at locations several wavelengths from the trailing edge (leech), but are important near the leech. It is shown that the induced-tension term in the governing P.D.E. derives from the in-plane kinetic energy of the flag motion.

Dynamically induced tension is shown to be important if the stiffness of the fabric is low: an order of magnitude criterion is presented.

1 Introduction

Flag flutter raises three fundamental questions:

1. Why does the flag flutter?
2. Why is the drag of a fluttering flag or banner much greater than that of a similar rigid vane?

3. What limits the amplitudes of a fluttering flag?

The first question was answered qualitatively by Thoma [1] when he pointed out that flow over a wavy surfaces produces an elevated pressure in the troughs and a reduced pressure over the crests, tending to increase the amplitudes. Sparenberg [2] confirmed that a traveling wave is generated.

The second question was raised by Fairthorne [3]. He observed that the increased drag varies directly with the mass-per-unit-area of the material, consistent with causation by the dynamics of the motion. Thoma [4] obtained the average tension in a waving rope, and linked it to the third question by pointing out that this dynamically induced tension tends to oppose the fluid-dynamic instability [1]. Our objective is to study this balance of forces.

Where the flag curves, any tension tends to flatten the flag, opposing pressure differences across the flag. These pressure differences are complementary to the flow field around the flag. Conversely, the flow field around the flag generates pressure forces normal to the flag, accelerating it; the resulting motions of the flag generate centrifugal forces which induce tension in the flag; and this tension opposes and ultimately limits the amplitudes of the flag motion.

This process dynamically transform normal (lift) forces on a flexible fabric into tension (drag) forces. It can be studied or measured either from the structural and from the fluid side:

- from the structural side, we can analyze the dynamics of the flag (as we will do below), or measure the drag forces at the flagpole; and
- from the fluid side, we can analyze the flow field, or measure the velocity profile in the wake.

The drag force must, of course, balance the momentum defect in the wake.

For the purpose of the initial physical analysis, the following simplifications will be made:

- A: The flag is perfectly *flexible*: the bending stiffness term is neglected.
- B: The flag is *inextensible*: the path length from luff to leech is constant.
- C: Gravity is neglected, and the deflections are uniform across the width.
- D: The flag is *wide* compared to wave-length: the flow-field is two-dimensional.
- E: Except for skin-friction calculations, the flow-field is potential flow.

The limitations introduced by these assumptions can be re-examined later.

2 Initial Stability

It has been proposed that flag flutter is caused either by vortex-shedding from the flagpole, or else by pressure-feedback from the vortex-street in the wake of a flat plate or sheet. However, observed flutter does not match either Strouhal frequency. Hence, our analysis looks for an instability phenomenon.

The governing equation of the flag for small deflections w as a function of time t and of distance x from the flagpole (luff) is

$$m_{flag} \frac{\partial^2 w}{\partial t^2} - T \frac{\partial^2 w}{\partial x^2} - \frac{\partial T}{\partial x} \frac{\partial w}{\partial x} + EI \frac{\partial^4 w}{\partial x^4} = \Delta p_{(t,x)} \quad (1)$$

where m_{flag} is the mass-per-unit-area of the flag, T is the tension-per-unit-width, and EI is the stiffness which we will neglect for now. Δp is the pressure difference generated by the flow field. In a paper on web spans [5] we have shown that the effect of a potential flow field can be replaced by aerodynamic mass terms resembling the “gyroscopic” inertia, Coriolis, and centrifugal coefficients in the Threadline Equation [6]

$$(m_{flag} + m_a) \frac{\partial^2 w}{\partial t^2} + 2m_a U_\infty \frac{\partial^2 w}{\partial t \partial x} + (m_a U_\infty^2 - T) \frac{\partial^2 w}{\partial x^2} - \frac{\partial T}{\partial x} \frac{\partial w}{\partial x} = 0 \quad (2)$$

where U_∞ is the far-field velocity of the surrounding air and m_a is the aerodynamically induced mass-per-unit-area. For slender webs, m_a is a function only of web width and air density ρ_{air} ; but for wide webs and sinusoidal deflections of wavelength λ , it becomes $m_a = \rho_{air} \lambda / \pi$. While this representation is appropriate for continuous web spans, it is imperfect near the trailing edge (leech) of a flag, but still useful for approximate analysis.

Tension $T > m_a U_\infty^2$ provides initial stability of a flexible flag. However, tension due to boundary-layer shear is small; at laminar Reynolds numbers, the tension-per-unit-width is

$$\frac{T_{drag}}{L \rho_{air} U_\infty^2} \cong 1.328 \sqrt{\frac{(\mu_{air} / \rho_{air})}{U_\infty L}} \left[\frac{\sqrt{L} - \sqrt{x}}{\sqrt{L}} \right] \quad (3)$$

which peaks at the leading edge, but falls towards zero as we approach the trailing edge, $x \rightarrow L$.

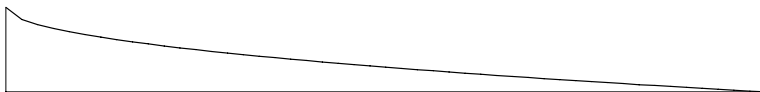


Figure 1: *Distribution of drag-induced tension as a function of location x*

At the leading (luff) edge, the tension is proportional to $U_\infty^{1.5}$ for laminar boundary layers (or to $U_\infty^{1.2}$ for turbulent boundary layers). We see that a

flag is unstable even at quite small U_∞ , at least near the trailing edge, unless we introduce some stiffness EI as in panel-flutter. Observations by Datta & Gottenberg [7] and Yamaguchi *et al.*[8] confirm that flexible flags begin to flutter at very low wind velocities.

3 Wave Form

Once flutter begins, additional tension is induced by the dynamic deflection w in the z -direction (normal to the initial plane of the flag). For the purpose of analysis, we postulate a deflection w which captures the essential features of the observed motion: a *traveling wave* within an envelope growing from a value of zero at the luff ($x = 0$) to the amplitude A at the leech ($x = L$), *e.g.*, in the form suggested by Thoma [1]

$$\begin{aligned} w &= \frac{A \sin(\alpha x/L)}{\sin(\alpha)} \cos(\omega t - \kappa x) \\ &= \frac{A}{2 \sin(\alpha)} \left[\sin\left(\omega t - \kappa x + \frac{\alpha}{L}x\right) - \sin\left(\omega t - \kappa x - \frac{\alpha}{L}x\right) \right] \end{aligned} \quad (4)$$

where the constant $\alpha \leq \pi/2$ is the shape parameter of the envelope. The simplest case, used by Uno [9], is to let $\alpha \rightarrow 0$, resulting in a *linearly increasing envelope* for the traveling wave

$$w = \frac{Ax}{L} \cos(\omega t - \kappa x) \quad (5)$$

where A is the maximum amplitude; x is the distance along the flag measured from the luff; L is the maximum value of x ; and the frequency of the waves is $f = \omega/2\pi$. In this first approximation, κ is taken to be a constant; therefore, the *wave-length is assumed constant* at $\lambda = 2\pi/\kappa$ and phase velocity $c = f\lambda = \omega/\kappa$ is also constant.

Experimental observations by Watanabe *et al.*[10] on flutter of sheets as well as slack edges of webs in paper machines, indicate that this description is appropriate over a wide range of air velocities. At very low velocities both Uno [9] and Watanabe *et al.*[10] observed similar behavior, but with a smaller number of waves within the length of the flag. At very high velocities, Taneda [11] observed an additional flapping motion at a higher frequency near the trailing edge, overlaid onto the basic flutter motion. In the presence of some amount of stiffness EI , both Taneda [11] and Watanabe *et al.*[10] observed partial nodes, indicating a certain amount of wave reflection at the trailing edge.

Similar wave forms have also been observed by Zhang *et al.*[12] on filaments in flowing soap films, which have been numerically simulated by Farnell, David, & Barton [13].

4 Time-averaged Tension

Thoma [4] analyzed an oscillating rope subjected to arbitrary normal forces (or a waving flag subjected to pressures). Writing V for velocity and T for tension, he derived a simple relationship for *average* tension as a function of distance s along the flag.

$$\frac{d\bar{T}}{ds} = \frac{m_{flag}}{2} \cdot \frac{d}{ds} (\overline{V^2}) \quad (6)$$

Integrating along the length L of the flag, with uniform mass-per-unit-length m_{flag} from luff ($s = 0$) to leech ($s = L$), the average value of the tension at the attachment is

$$\bar{T}_{luff} = \frac{1}{2} m_{flag} \overline{V^2}_{leech} \quad (7)$$

Inserting our simple wave form and evaluating it near the tip ($x \cong L$)

$$\overline{V^2}_{leech} \cong \frac{A^2 \omega^2}{2} \quad (8)$$

we obtain the total dynamically-induced drag at the flagpole

$$\bar{T}_{luff} \cong \frac{m_{flag}}{2} \cdot \frac{A^2 \omega^2}{2} \quad (9)$$

Starting with Fairthorne [3], practical observations indicate that this is generally substantially greater than skin-friction drag.

Similarly, we can obtain the *time-averaged tension distribution* as a function of x

$$\begin{aligned} \bar{T}_{(x)} &= \frac{m_{flag}}{2} \cdot (\overline{V^2}_{leech} - \overline{V^2}_{(x)}) \\ &\cong \left(\frac{m_{flag}}{2} \cdot \frac{A^2 \omega^2}{2} \right) \left(1 - \frac{x^2}{L^2} \right) \end{aligned} \quad (10)$$

showing that the dynamically induced tension is distributed much more broadly than drag-induced tension.

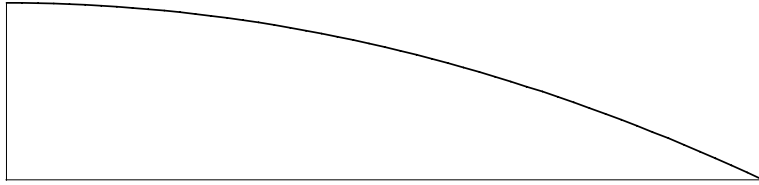


Figure 2: *Distribution of dynamically induced tension as a function of location.*

5 Tension Fluctuations

Using *Scientific WorkPlace* [14], which uses *Maple* as a Computer Algebra System, we can relate the path length s of the wave to coordinate x

$$\frac{ds}{dx} = \sqrt{1 + \left(\frac{dw}{dx}\right)^2} \quad (11)$$

The u -deflection in the (negative) x -direction (parallel to the free-stream velocity) is $u = x - s$. The position of an element of the flag is described by the w -deflection normal to the reference plane, plus the u -deflection in the reference plane of the flag. For moderate deflections and slopes, $(dw/dx)^2 \ll 1$, we can approximate the path length expression with the first two terms of the binomial expansion

$$\frac{ds}{dx} \cong 1 + \frac{1}{2} \left\{ \frac{A}{L} [\cos(\omega t - \kappa x) + x\kappa \sin(\omega t - \kappa x)] \right\}^2 \quad (12)$$

which simplifies the algebra considerably. We integrate, expand the terms to separate time and space variables, and obtain the longitudinal deflection and acceleration. Combining this with the transverse acceleration to obtain the acceleration vector, and relating it to the direction cosines of the flag itself, the change in tension with location is described by

$$\frac{dT}{dx} \cong - \left(\frac{A}{L}\right)^2 m_{flag} \frac{\omega^2}{\kappa} \left\{ \begin{array}{l} \frac{1}{2}\kappa x + \frac{1}{2} \cos \kappa x \sin \kappa x \\ - [\cos \kappa x \sin \kappa x] \cos^2 \omega t \\ - [\sin^2 \kappa x] \cos \omega t \sin \omega t \end{array} \right\} \quad (13)$$

which we can integrate to obtain tension

$$T \cong \left(\frac{A}{L}\right)^2 m_{flag} \frac{\omega^2}{\kappa^2} \left\{ \begin{array}{l} \frac{1}{4}(\kappa L)^2 - \frac{1}{4}(\kappa x)^2 \\ + [\frac{1}{8} \cos 2\kappa L - \frac{1}{8} \cos 2\kappa x] \cos 2\omega t \\ + [\frac{1}{8} \sin 2\kappa L - \frac{1}{8} \sin 2\kappa x - \frac{1}{4}\kappa L + \frac{1}{4}\kappa x] \sin 2\omega t \end{array} \right\} \quad (14)$$

where the expression in the curly brackets reaches a *maximum value* at the luff, where $x = 0$

$$\left\{ \frac{1}{4}(\kappa L)^2 + \frac{1}{8} \sqrt{2 - 2 \cos 2\kappa L - 4\kappa L \sin 2\kappa L + 4(\kappa L)^2 \cos(2\omega t - \phi)} \right\} \quad (15)$$

The value and distribution of the *time-averaged* tension have already been shown in the previous section; the amplitude of the *fluctuations* in tension at the luff is

$$\left(\frac{A}{L}\right)^2 m_{flag} \frac{\omega^2}{\kappa^2} \left\{ \frac{1}{8} \sqrt{2 - 2 \cos 2\kappa L - 4\kappa L \sin 2\kappa L + 4(\kappa L)^2 \cos(2\omega t - \phi)} \right\} \quad (16)$$

We can determine bounds as follows:

$$\frac{1}{4}\sqrt{(\kappa L)^2 - \kappa L} \leq \frac{1}{8}\sqrt{2 - 2\cos 2\kappa L - 4\kappa L \sin 2\kappa L + 4(\kappa L)^2} \leq \frac{1}{4}(\kappa L + 1) \quad (17)$$

We conclude that the amplitude of the fluctuations is guaranteed to be less than the average if $L > \lambda/4$. This condition is met by typical flags, which are several wave-lengths long. When the flag is many wave-lengths long ($\kappa L \gg 1$), the fluctuations approach $\kappa L/4$, which is $1/\kappa L$ of the average value.

6 Governing Equation

Having demonstrated the importance of the dynamically-induced tension, we expand the Equation 1 to include non-linear structural terms. Using the Hamilton's Principle approach outlined by Païdoussis [15], and using the curvilinear coordinate s along the path of the inextensible flag

$$\begin{aligned} & m_{flag} \frac{\partial^2 w}{\partial t^2} + EI \left\{ \frac{\partial^4 w}{\partial s^4} \left[1 + \left(\frac{\partial w}{\partial s} \right)^2 \right] + 4 \frac{\partial w}{\partial s} \frac{\partial^2 w}{\partial s^2} \frac{\partial^3 w}{\partial s^3} + \left(\frac{\partial^2 w}{\partial s^2} \right)^3 \right\} \\ & - \frac{\partial^2 w}{\partial s^2} \left\{ T_{drag} \left[1 + \frac{3}{2} \left(\frac{\partial w}{\partial s} \right)^2 \right] + m_{flag} \int_s^L \int_0^s \left(\left(\frac{\partial^2 w}{\partial t \partial s} \right)^2 + \frac{\partial w}{\partial s} \frac{\partial^3 w}{\partial t^2 \partial s} \right) ds ds \right\} \\ & - \frac{\partial w}{\partial s} \left\{ \frac{\partial T_{drag}}{\partial s} \left[1 + \frac{1}{2} \left(\frac{\partial w}{\partial s} \right)^2 \right] + m_{flag} \int_0^s \left(\left(\frac{\partial^2 w}{\partial t \partial s} \right)^2 + \frac{\partial w}{\partial s} \frac{\partial^3 w}{\partial t^2 \partial s} \right) ds \right\} \\ & = \Delta p \end{aligned} \quad (18)$$

The integral terms, generated by the in-plane component of kinetic energy, can be seen to correspond to dynamically induced tension and tension-gradient terms.

7 Conclusion

We learn that we cannot neglect in-plane kinetic energy just because it is small compared to out-of-plane kinetic energy: the terms generated by in-plane motion compete with skin-friction T_{drag} and stiffness EI terms. We must assess the importance of $T\partial^2 w/\partial x^2$ by comparison with $EI\partial^4 w/\partial x^4$ at the appropriate wavelength.

Acknowledgements: This work was made possible by an Alexander von Humboldt Research Award, and was carried out with suggestions and encouragement from Prof. Peter Hagedorn at T.U. Darmstadt in Germany.

References

- [1] Dieter Thoma, “Warum flattert die Fahne”, *Mitteilungen des Hydraulischen Instituts der Technischen Hochschule München*, Heft 9 (1939), pages 30–34.
- [2] J.A. Sparenberg, “On the waving motion of a flag”, *Proc. Koninklijke Nederlandse Akademie van Wetenschappen, Series B: Physical Sciences*, Vol. LXV (1962), Mechanics.
- [3] R.A. Fairthorne, “Drag of Flags”, *Aeronautical Research Committee (ARC) Reports and Memoranda No. 1345 (Ae. 477)*, pages 887–891, HMSO, London 1930.
- [4] D. Thoma, “Das schlenkernde Seil” (The oscillating rope), *Z. Angew. Math. Mech. (ZAMM)*, Band 19, Nr. 5 (October 1939), pages 320–321.
- [5] Y.B. Chang, S.J. Fox, D.G. Lilley, & P.M. Moretti, “Aerodynamics of moving belts, tapes, and webs”, *ASME Machinery Dynamics and Element Vibration DE-Vol. 36* (Sept. 1991), ASBN 0-7918-0627-8, pages 33–40.
- [6] Peter M. Moretti, *Modern Vibrations Primer*, CRC Press, Boca Raton, FL 33431, ©2000, ISBN 0-8493-2038-0, page 302.
- [7] S.K. Datta & W.G. Gottenberg, “Instability of an elastic strip hanging in an airstream”, *Trans. ASME, J. of Applied Mechanics*, March 1975, pp 195–198.
- [8] Nobuyuki Yamaguchi, T. Sekiguchi, K. Yokota, & Y. Tsujimoto, “Flutter limits and behavior of a flexible thin sheet in high-speed flow—II. Experimental results ...”, *Trans. ASME, J. of Fluids Engineering*, Vol. 122 (March 2000), pp 65–83.
- [9] Minuro Uno, “Fluttering of flexible bodies”, *Journal of the Textile Machinery Society of Japan*, Vol. 19 (1973), No. 4/5, pages 103–109.
- [10] Y. Watanabe, S. Suzuki, M. Sugihara, & Y. Sueoka, “An experimental study of paper flutter”, *J. of Fluids and Structures*, Vol 16 (2002), No. 4, pp 529–560.
- [11] Sadatoshi Taneda, “Waving motion of flags”, *Journal of the Physical Society of Japan*, Vol 24, No. 2 (Feb. 1968), pages 392–401.
- [12] Jun Zhang, S. Childress, A. Libchaber, & M. Shelley, “Flexible filaments in a flowing soap film as a model for one-dimensional flags in a two-dimensional wind”, *Nature*, Vol. 408 (2000), pages 835–839.
- [13] D.J.J. Farnell, T. David, & D.C. Barton, “Numerical simulation of a filament in a flowing soap bubble”, correspondent Prof. David, Dept. Mech. Engrg., University of Canterbury, Christchurch, New Zealand; submitted to *Int. Jour. Num. Methods in Fluids*, 2003.
- [14] <http://www.mackichan.com/>
- [15] Michael P. Paidoussis, *Fluid-Structure Interactions: Slender Structures and Axial Flow Volume 1*, Academic Press, San Diego, CA, 1998, ISBN 0-12-544360-9.